International Journal of Thermophysics, Vol. 25, No. 5, September 2004 (© 2004)

Combined DSC and Pulse-Heating Measurements of Electrical Resistivity and Enthalpy of Platinum, Iron, and Nickel[1]

B. Wilthan,[2] C. Cagran,[2] and G. Pottlacher[2,3]

Measurements of the enthalpy, electrical resistivity, and specific heat capacity as a function of temperature starting from the solid state up into the liquid phase for Fe, Ni, and Pt are presented. Two different measurement approaches have been used within this work: an ohmic pulse-heating technique, which allows – among others – the measurement of enthalpy, specific heat capacity, and electrical resistivity up to the end of the stable liquid phase, and a differential–scanning–calorimetry technique (DSC) which enables determination of specific heat capacity from near room temperature up to 1500 K. The microsecond ohmic pulse-heating technique uses heating rates up to $10^8 \mathrm{K \cdot s^{-1}}$ and thus is a dynamic measurement, whereas the differential–scanning–calorimetry technique uses heating rates of typically $20 \mathrm{K \cdot min^{-1}}$ and can be considered as a quasi-static process. Despite the different heating rates both methods give good agreement of the thermophysical data within the stated uncertainties of each experiment. Results on the metals Fe, Ni, and Pt are reported. The enthalpy and resistivity data are presented as a function of temperature and compared to literature values.

KEY WORDS: differential scanning calorimetry; electrical resistivity; enthalpy; iron; nickel; platinum; pulse-heating; specific heat.

1. INTRODUCTION

Thermophysical property data such as enthalpy and electrical resistivity as a function of temperature have been measured for metals and alloys for

[1]Paper presented at the Fifteenth Symposium on Thermophysical Properties, June 22–27, 2003, Boulder, Colorado, U.S.A.

[2]Institut für Experimentalphysik, Technische Universität Graz, Petersgasse 16, A–8010 Graz, Austria.

[3]To whom correspondence should be addressed. Email: pottlacher@tugraz.at

0195-928X/04/0900-1519/0

many years at the Institut für Experimentalphysik in Graz by using various fast pulse-heating techniques at different time scales (heating rates of 10^8–10^9 K·s^{-1}) [1]. For our pulse-heating experiments on wire samples, the temperature is determined by means of fast optical pyrometers, which have a response time of about 100 ns. These monochromatic instruments may use two different detectors, namely a Si diode or an InGaAs diode. Since monochromatic pyrometers usually are "self-calibrated" using the plateau of the melting transition of the investigated metal, high sensitivity is desirable. A wide temperature range for a single set of measurements is possible with the use of a fast operational amplifier with a linear output. When using a fast optical pyrometer to measure the temperature of samples under rapid-heating conditions, several factors limit the lower cut-off temperature. For a short rise time the active area of the device has to be very small, e.g., 1 mm × 1 mm; also, the interference will limit the amount of light that reaches the detector. Because of shielding reasons, the pyrometer has to be housed in a shielded box, and the light of the radiating sample is conducted to it via optical light-guides; finally, there are losses due to reflection at the windows of the experimental chamber and at the lenses of the pyrometer, which all together strongly will decrease the flux of light that finally reaches the detector and result in a lowest detectable temperature of our pyrometers of about 1200–1500 K. Therefore, all thermophysical properties published earlier, e.g., Refs. 1 and 2, started at temperatures between 1200 and 1500 K.

Other than the pyrometric signal, all other basic measurements are electrical signals (current through the sample, voltage drop across the specimen) and thus not limited by the lower cut-off temperature. Therefore, we are able to measure these electrical signals over the entire range covered by the pulse-heating experiment starting from room temperature up to the end of the stable liquid phase.

As a result, evaluated thermophysical properties like enthalpy and electrical resistivity can generally be calculated over the entire temperature range, but the onset temperature of the pyrometers (of about 1200–1500 K) limits the possibility to report these quantities versus temperature to the range above the pyrometer onset, which is, in fact, a strong limitation.

To overcome this limitation and to obtain temperature dependencies for these quantities below the onset temperature of the pyrometers, a differential scanning calorimeter (DSC) Netzsch DSC 404 was added to our setup and incorporated into the basic measurement routines for data in the temperature range of about 500–1500 K. The DSC is able to perform accurate specific heat capacity measurements in the above mentioned temperature range. The results are combined with those of the

pulse-heating experiments by using the enthalpy versus temperature dependence of the DSC to expand the temperature range of the pulse-heating data. Thus, temperature dependencies of all thermophysical properties can now be extended down to the DSC onset temperature of about 500 K.

2. MEASUREMENTS

2.1. Pulse-heating with Microsecond Time Resolution

The optics of the pyrometer views an area of 0.2 mm × 10 mm of the pulse-heated sample surface (sample dimensions: 50 mm length, 0.5 mm diameter) with a 1:1 magnification onto the rectangular entry slit of an optical waveguide. The interference filter with a center wavelength of 650 nm and a half power bandwidth of 37 nm is in front of the entry slit of the waveguide. The light delivered by this waveguide is detected by a Si-photodiode and amplified with a fast amplifier (bandwidth 1 MHz). The intensity signal J can be expressed as

$$J(\lambda, T) = g\sigma(\lambda)\tau(\lambda)\varepsilon_\lambda(\lambda, T)\frac{c_1}{\lambda^5\left[e^{\frac{c_2}{\lambda \cdot T}} - 1\right]}, \tag{1}$$

where the symbols are defined as follows: g, geometry factor; σ, sensitivity of electronics and diode; λ, wavelength; τ, transmission of optic and optical waveguide; ε_λ, normal spectral emissivity, c_1 and c_2, first and second radiation constant; and T, temperature.

By forming ratios of the measured radiance intensity at melting $J(T_M)$ and the measured radiance intensity $J(T)$ at temperature T, one obtains the unknown temperature T with the melting temperature of the investigated material as the calibration point:

$$T = \frac{c_2}{\lambda \ln\left\{1 + \frac{J_m(T_M)\varepsilon(\lambda, T)}{J(T)\varepsilon(\lambda, T_M)}\left[\exp\left(\frac{c_2}{\lambda T_M}\right) - 1\right]\right\}}, \tag{2}$$

where $\varepsilon(\lambda, T)$ is the emissivity of the liquid sample and $\varepsilon(\lambda, T_M)$ is the emissivity at the melting temperature. For emissivity dependencies of liquid metals, see, e.g., Ref. 3.

The temperature range covered by the optical pyrometer is from about 1200 up to about 5000 K, depending on the material under investigation. Thus, the experiments extend far into the metal's liquid phase. The stability limit of the pulse-heated wire sample for this type of experiment is the boiling of the sample. During one fast pulse experiment by measuring the current through the sample, the voltage drop across it,

and the radiation temperature, one may obtain data for the enthalpy, temperature, and electric resistivity as the specimen rapidly passes through a wide range of states from room temperature up into the liquid phase. From these quantities the specific heat at constant pressure, the thermal conductivity, and thermal diffusivity may be calculated. For more details on the experiment and on data reduction, see, e.g., Ref. 1.

2.2. DSC Measurements

The DSC can be used primarily for measurements of the heat capacity of the sample (5.2 mm diameter and 0.5 mm height) in the temperature range from 500 to 1500 K. The sample is measured relative to a second, inert sample of approximately the same heat capacity. One experiment consists usually of three separate runs: a scan with two empty pans, a scan with one pan containing a sapphire reference sample, and finally a scan with the sample in the same pan where the reference sample was previously. The heat capacity as a function of temperature of the sample under investigation, $c_p(T)$, is obtained by using the following equation:

$$c_p(T) = c_p^{\mathrm{r}}(T)\frac{m^{\mathrm{r}}}{m}\frac{\Delta_3 - \Delta_1}{\Delta_2 - \Delta_1}, \tag{3}$$

where Δ_1, Δ_2, and Δ_3 are the three DSC signals with empty pans, the signal of the reference, and the signal of the sample, respectively. m^{r} and m are the masses of the reference and the sample, respectively, and c_p^{r} is the heat capacity of the reference.

Using this heat capacity $c_p(T)$ obtained with DSC measurements, one is able to calculate the enthalpy of the specimen by integrating the heat capacity signal with respect to temperature and adding a constant enthalpy from T = 473 K to room temperature to the result:

$$H_{298}(T) = \int_{473}^{T} c_p(T)dT + (473 - 298)c_p(473), \tag{4}$$

where $H(T)$ is the enthalpy and c_p is the specific heat capacity. The assumption in Eq. (4) of a constant heat capacity between 298 and 473 K is taken into consideration for the uncertainty of the enthalpy values.

Therefore, the enthalpy versus temperature dependence for a given material can be calculated directly from DSC measurements. This enthalpy-temperature dependence can further be used to obtain the inverse dependence, temperature versus enthalpy. With this result, we are able to extend our electrical measurements (i.e., enthalpy or electrical resistivity) of the

pulse-heating experiment to lower temperatures by combining the temperature scale from the DSC (temperature versus enthalpy) with the electrical measured properties versus enthalpy. It has to be noted that the above mentioned procedure is only applicable as long as there are no phase transitions in the solid sate of the material under investigation. Phase transitions can easily be observed with DSC measurements, but can be wholly or partially suppressed under pulse-heating conditions as applied within this experiment, due to the extreme high heating rates of $10^8\,\mathrm{K\cdot s^{-1}}$. This procedure enables us to extend the results for enthalpy versus temperature and resistivity versus temperature to lower temperature regions, starting now at the onset temperature of the DSC (500 K). Up to now access to these temperature regions when using pulse-heating techniques was only possible by experiments with millisecond time resolution [4].

3. RESULTS

We used the following melting temperatures for data evaluation: nickel: 1728 K [5], iron: 1808 K [6], and platinum: 2042 K [7].

3.1. Platinum

The platinum wires used for the experiments were fabricated by "Advent Research" with a given purity of 99.99+%.

In Fig. 1 the specific enthalpy versus temperature results for platinum is plotted. In the temperature range $473\,\mathrm{K} < T < 1573\,\mathrm{K}$ we obtain from our DSC measurements the following fit:

$$H(T) = -38.689 + 0.127T + 1.344 \times 10^{-5}T^2, \tag{5}$$

where H is in $\mathrm{kJ\cdot kg^{-1}}$ and T is in K.

The linear fit for solid platinum in the temperature range $1700\,\mathrm{K} < T < 2040\,\mathrm{K}$ is obtained from 11 independent pulse-heating measurements:

$$H(T) = -96.075 + 0.180T. \tag{6}$$

For the liquid in the temperature range $2045\,\mathrm{K} < T < 2830\,\mathrm{K}$ we obtain again from 11 pulse-heating measurements:

$$H(T) = 1.636 + 0.187T. \tag{7}$$

Figure 2 presents the specific electrical resistivity with the initial geometry, $\rho_{\mathrm{el},IG}$, not compensated for thermal expansion, as a function of temperature for platinum. In the temperature range $473\,\mathrm{K} < T < 1573\,\mathrm{K}$, we obtain

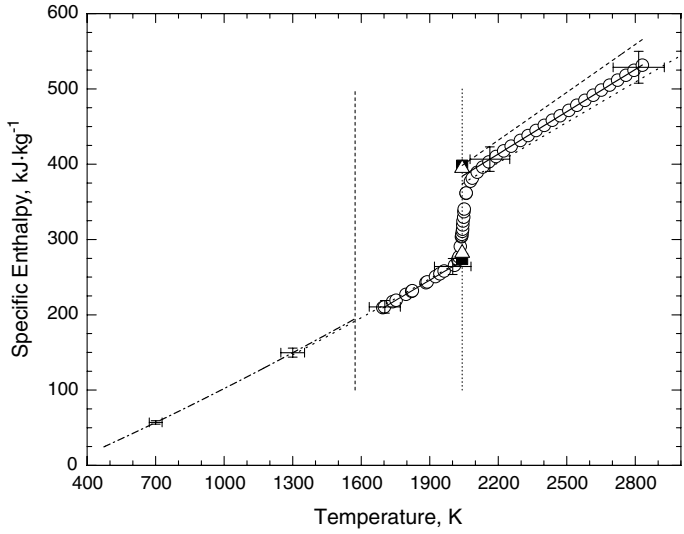

Fig. 1. Specific enthalpy versus temperature for platinum. Open circles represent measured pulse-heating data from this work (average of 11 measurements). Solid lines: linear least-squares fits to mean values of measured data; filled squares: values at the beginning and end of melting from [8]; dashed line: literature values for the liquid phase from [8]; vertical dashed line: end of values measured and calculated with DSC data (1573 K); vertical dotted line: melting temperature (2042 K); open triangle: literature value from [9] at the melting temperature; dotted line: literature values from [10]; dashed-dotted line: data from this work (DSC measurements).

from our DSC measurements the following fit:

$$\rho_{\mathrm{el},IG}(T) = -0.018 + 4.464 \times 10^{-4} T - 6.955 \times 10^{-8} T^2, \tag{8}$$

where $\rho_{\mathrm{el},IG}$ is in $\mu\Omega$·m and T is in K.

The linear fit to our values for the solid in the temperature range $1740\,\mathrm{K} < T < 2042\,\mathrm{K}$ is

$$\rho_{\mathrm{el},IG}(T) = 0.155 + 2.229 \times 10^{-4} T \tag{9}$$

and for the liquid in the temperature range $2042\,\mathrm{K} < T < 2900\,\mathrm{K}$

$$\rho_{\mathrm{el},IG}(T) = 0.854 + 2.713 \times 10^{-5} T. \tag{10}$$

In Fig. 2 the specific electrical resistivity with the volume expansion included, $\rho_{\mathrm{el,VOL}}$, is also plotted as a function of temperature. The polynomial fit to our specific electrical resistivity with volume expansion

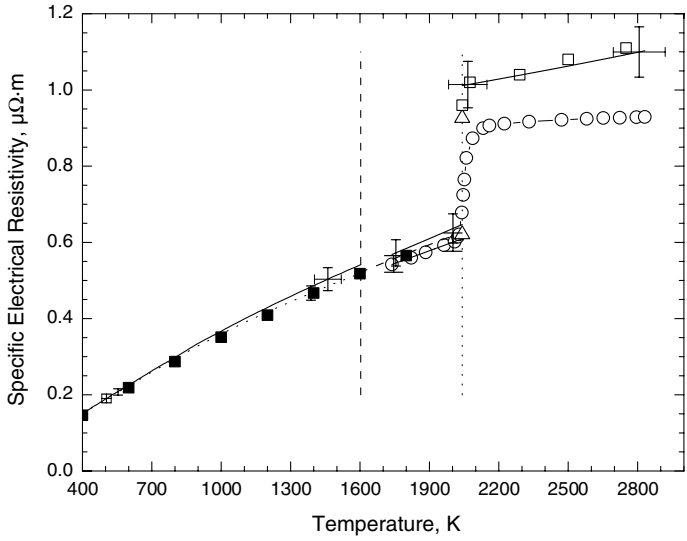

Fig. 2. Electrical resistivity of platinum resistivity without taking actual volume in account, and with volume expansion taken into consideration, versus temperature for platinum. Open circles represent measured pulse-heating data with the initial geometry from this work (average of 11 measurements). Filled squares: literature values from [11]; open triangles: values from [9]; dotted line: measured from this work with temperatures from DSC without taking actual volume in account. Solid line: electrical resistivity adapted for volume expansion from Refs. 12 and 13. Lines are least-squares fits to measured data. Vertical dashed line: end of values measured and calculated with DSC data (1573 K); vertical dotted line: melting temperature (2042 K); dashed line: literature values from [14] without volume correction.

included, $\rho_{\mathrm{el,VOL}}$, data of expansion the solid from [13] in the temperature range $473\,\mathrm{K} < T < 1600\,\mathrm{K}$ is

$$\rho_{\mathrm{el,VOL}}(T) = -0.01633 + 4.39347 \times 10^{-4} T - 5.69652 \times 10^{-8} T^2, \quad (11)$$

and for $1740\,\mathrm{K} < T < 2042\,\mathrm{K}$ is

$$\rho_{\mathrm{el,VOL}}(T) = 0.161 + 2.132 \times 10^{-4} T + 1.219 \times 10^{-8} T^2. \quad (12)$$

For the liquid expansion data [12] in the temperature range $2042\,\mathrm{K} < T < 2900\,\mathrm{K}$, the fit is

$$\rho_{\mathrm{el,VOL}}(T) = 0.842 + 5.926 \times 10^{-5} T + 1.154 \times 10^{-8} T^2. \quad (13)$$

The effect of the volume expansion on resistivity is shown as an example for platinum. For all other materials only the resistivity at the initial geometry will be presented, as the compensation of volume expansion shifts the resistivity to higher values and can be done with the corresponding volume expansion data available in the literature.

3.2. Nickel

The wires used for the pulse-heating experiments were fabricated with a given purity of 99.98% by "Advent Research." The cylindrical samples for the DSC measurements have a purity of 99.99+% (Ca – 10 ppm, Mg – 0.3 ppm) and were obtained from Aldrich Chemical Company.

Figure 3 presents the enthalpy versus temperature results for nickel. In the temperature range $473\,\mathrm{K} < T < 1270\,\mathrm{K}$ we obtain from our DSC-measurements the following fit:

$$H(T) = -166.644 + 0.546T + 2.394 \times 10^{-6} T^2, \tag{14}$$

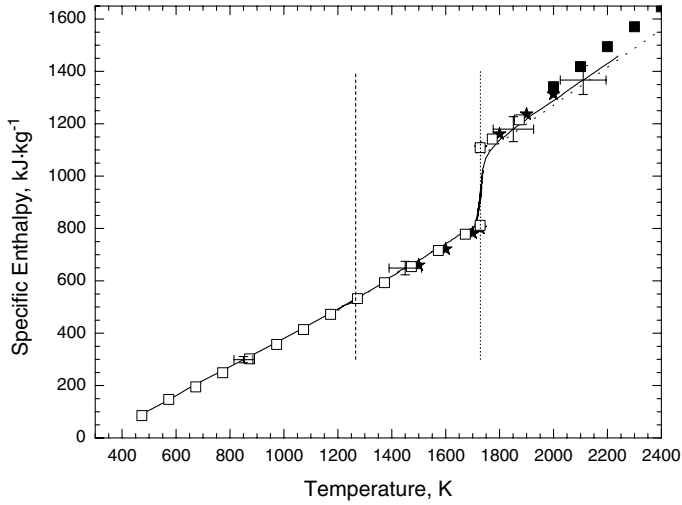

Fig. 3. Specific enthalpy versus temperature for nickel. Solid lines represent measured data from this work; vertical dashed line: end of values measured and calculated with DSC data (1266 K); vertical dotted line: melting temperature (1729 K); open squares: literature values from [15]; filled stars: values from [16]; filled squares: literature values for the liquid phase from [17]; dotted line: data from [18].

the linear fit for solid nickel obtained by pulse-heating in the temperature range $1200\,\mathrm{K} < T < 1715\,\mathrm{K}$ is

$$H(T) = -272.961 + 0.634T, \tag{15}$$

and for the liquid in the temperature range $1740\,\mathrm{K} < T < 2240\,\mathrm{K}$,

$$H(T) = -151.913 + 0.720T. \tag{16}$$

Figure 4 depicts the electrical resistivity with the initial geometry versus temperature for nickel. The change of the slope in this figure is due to a ferromagnetic to paramagnetic transformation in the nickel sample.
In the range $473\,\mathrm{K} < T < 627\,\mathrm{K}$ we obtain from the DSC:

$$\rho_{\mathrm{el},IG}(T) = -0.042 + 2.080 \times 10^{-4}T + 5.126 \times 10^{-7}T^2 \tag{17}$$

and in the range $627\,\mathrm{K} < T < 1270\,\mathrm{K}$,

$$\rho_{\mathrm{el},IG}(T) = -0.181 + 0.001T - 8.197 \times 10^{-7}T^2 + 2.351 \times 10^{-10}T^3. \tag{18}$$

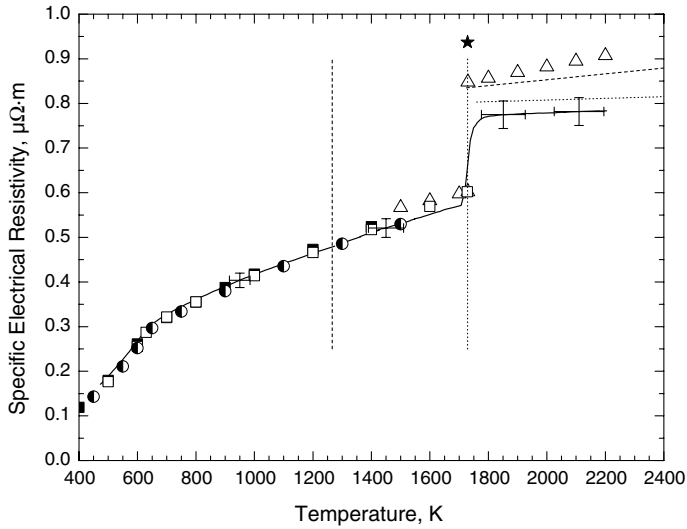

Fig. 4. Electrical resistivity of (with initial geometry) versus temperature. Solid line represents measured data from this work; vertical dashed line: end of values measured and calculated with DSC data (1266 K); vertical dotted line: melting temperature (1729 K); filled squares: values from [11] in the solid phase; half-filled circles: data from [19]; open squares: values from [20]; open triangles: values from [16]; dashed line: values for the liquid phase from [21]; dotted line: data from [18]; filled star: value at melting temperature in the liquid phase from [22].

By means of pulse-heating we obtain in the range $1300\,\mathrm{K} < T < 1715\,\mathrm{K}$,

$$\rho_{\mathrm{el},IG}(T) = 0.094 + 3.764 \times 10^{-4} T - 5.644 \times 10^{-8} T^2 \tag{19}$$

and in the range $1750\,\mathrm{K} < T < 2200\,\mathrm{K}$:

$$\rho_{\mathrm{el},IG}(T) = 0.728 + 2.546 \times 10^{-5} T. \tag{20}$$

3.3. Iron

The iron wires from "Advent Research" with a purity of 99.5% were also used as received. The DSC samples have a purity of 99.99%.

In Fig. 5 the enthalpy versus temperature results for iron are presented. For the temperature range from $473\,\mathrm{K} < T < 1270\,\mathrm{K}$ our DSC measurements are presented in Table I, as the data can not be described by a polynomial fit (also a higher-order polynomial fit would cause unacceptable differences in the accuracy of the graph).

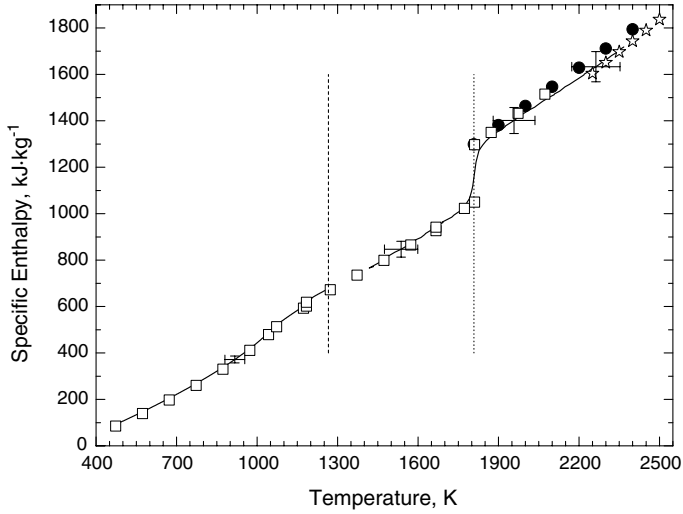

Fig. 5. Specific enthalpy versus temperature for iron. Solid lines represent measured data from this work; vertical dashed line: end of values measured and calculated with DSC data (1266 K); vertical dotted line: melting temperature (1808 K); open squares: literature values from [15]; filled circles: data from the liquid phase from [23]; open stars: high temperature values from [17].

Table I. Experimental DSC data for Enthalpy Versus Temperature for Solid Iron

T (K)	H (kJ·kg^{-1})	T (K)	H (kJ·kg^{-1})
473	92.330	1034	478.620
500	106.625	1050	497.253
550	133.844	1066	513.856
600	162.086	1100	543.701
650	191.385	1150	583.496
700	221.806	1187	611.617
750	253.464	1191	615.813
800	286.575	1200	630.727
850	321.450	1205	637.155
900	358.630	1214	644.517
950	398.821	1250	667.282
1000	443.645	1270	679.802

The linear fit for solid iron in the temperature range $1420\,\mathrm{K} < T < 1790\,\mathrm{K}$ obtained by pulse-heating is

$$H(T) = -276.650 + 0.732T \tag{21}$$

and for the liquid in the temperature range $1830\,\mathrm{K} < T < 2370\,\mathrm{K}$ we obtain

$$H(T) = -107.306 + 0.770T. \tag{22}$$

Figure 6 depicts the electrical resistivity versus temperature results for iron. In the range $473\,\mathrm{K} < T < 1000\,\mathrm{K}$ by means of DSC we obtain

$$\rho_{\mathrm{el},IG}(T) = 0.015 + 1.998 \times 10^{-4}T + 5.433 \times 10^{-7}T^2 + 1.935 \times 10^{-10}T^3 \tag{23}$$

and in the range $1000\,\mathrm{K} < T < 1270\,\mathrm{K}$,

$$\rho_{\mathrm{el},IG}(T) = -20.603 + 0.053T - 4.269 \times 10^{-5}T^2 + 1.161 \times 10^{-8}T^3. \tag{24}$$

By pulse-heating we obtain in the solid range $1250\,\mathrm{K} < T < 1790\,\mathrm{K}$,

$$\rho_{\mathrm{el},IG}(T) = 0.591 + 6.594 \times 10^{-4}T - 1.648 \times 10^{-7}T^2 \tag{25}$$

and in the liquid range $1830\,\mathrm{K} < T < 2370\,\mathrm{K}$

$$\rho_{\mathrm{el},IG}(T) = 1.232 + 2.342 \times 10^{-5}T. \tag{26}$$

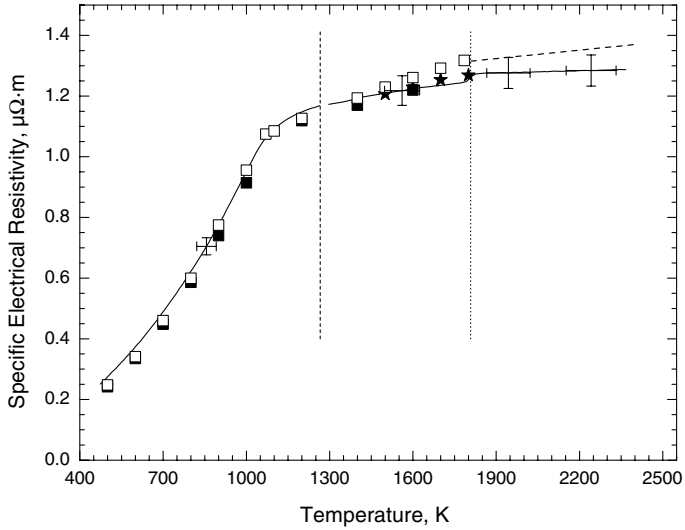

Fig. 6. Electrical resistivity of iron (with initial geometry) versus temperature. Solid line represents measured pulse-heating data from this work; vertical dashed line: end of values measured and calculated with DSC data (1266 K); vertical dotted line: melting temperature (1808 K); open squares: literature data from [24]; filled squares: values for the solid phase from [11]; filled stars: data from [25]; dashed line: data for liquid iron from [21].

4. DISCUSSION

For solid platinum we obtain a c_p value of $180\,\mathrm{J\cdot kg^{-1}\cdot K^{-1}}$ in the range from 1700 to 2040 K. Seville [26] reports a value of $187.5\,\mathrm{J\cdot kg^{-1}\cdot K^{-1}}$ at 1850 K, Righini and Rosso [14] report a value of $189\,\mathrm{J\cdot kg^{-1}\cdot K^{-1}}$ at 2000 K, and at the onset of melting, Hultgren et al. [10] report $179.6\,\mathrm{J\cdot kg^{-1}\cdot K^{-1}}$. For the liquid we acquire a c_p value of $187\,\mathrm{J\cdot kg^{-1}\cdot K^{-1}}$, Margrave [27] reports a value of $186.7\,\mathrm{J\cdot kg^{-1}\cdot K^{-1}}$, and Chaudhuri et al. [28] report a value of $186\,\mathrm{J\cdot kg^{-1}\cdot K^{-1}}$ obtained by levitation calorimetry. Hixson and Winkler [8] report $211.9\,\mathrm{J\cdot kg^{-1}\cdot K^{-1}}$ at a pressure of 2000 bar obtained by pulse-heating and Hultgren et al. [10] recommend $178.1\,\mathrm{J\cdot kg^{-1}\cdot K^{-1}}$. The measured values show very good agreement with the literature values for both the solid and the liquid phases within the estimated uncertainties.

As shown in Fig. 1, we obtain a value of $(112 \pm 9)\,\mathrm{kJ\cdot kg^{-1}}$ for the melting enthalpy ΔH, while Hultgren et al. [10] recommend $100.8\,\mathrm{kJ\cdot kg^{-1}}$.

For a detailed discussion of the melting enthalpy of platinum, see Ref. 30.

At the onset of melting (2042 K), which is indicated by a vertical dotted line in Fig. 2, we obtain a value of $0.610\,\mu\Omega\cdot\mathrm{m}$ for the electrical resistivity of platinum, and at the end of melting, a value of $0.909\,\mu\Omega\cdot\mathrm{m}$; thus, an increase of $\Delta\rho = 0.299\,\mu\Omega\cdot\mathrm{m}$ at melting is observed. At 2000 K, Righini and Rosso [14] report a value of $0.617\,\mu\Omega\cdot\mathrm{m}$, and Martynyuk and Tsapkov [9] report for the onset of melting $0.621\,\mu\Omega\cdot\mathrm{m}$ and for the end of melting $0.926\,\mu\Omega\cdot\mathrm{m}$. For the case when volume expansion is taken into account for the resistivity values, at the onset of melting we obtain a value of $0.647\,\mu\Omega\cdot\mathrm{m}$ and at the end of melting a value of $1.012\,\mu\Omega\cdot\mathrm{m}$. An increase of $\Delta\rho = 0.365\,\mu\Omega\cdot\mathrm{m}$ at melting is observed. Platinum was the only material where we compared the measured resistivity results to literature values for the initial geometry and with volume expansion considered. All measured values show excellent agreement with literature values. Based on these results, we suggest that platinum could be used as a calibration standard for pulse-heating circuits regarding measurements of enthalpy and resistivity.

For solid nickel using pulse-heating in the temperature range $1200\,\mathrm{K} < T < 1715\,\mathrm{K}$, we obtain a c_p of $634.4\,\mathrm{J\cdot kg^{-1}\cdot K^{-1}}$, and for the liquid in the temperature range $1740\,\mathrm{K} < T < 2240\,\mathrm{K}$, a c_p value of $797.9\,\mathrm{J\cdot kg^{-1}\cdot K^{-1}}$. Cezairliyan and Miiller [29] report $c_p(1700\,\mathrm{K}) = 654.8\,\mathrm{J\cdot kg^{-1}\cdot K^{-1}}$, and Hultgren et al. [10] give $c_p\ (1726\,\mathrm{K}) = 734.8\,\mathrm{J\cdot kg^{-1}\cdot K^{-1}}$. The measured results show good agreement with literature values.

As shown in Fig. 3, we obtain a value of $(276 \pm 22)\ \mathrm{kJ\cdot kg^{-1}}$ for the melting enthalpy ΔH and Hultgren et al. [10] recommend $298\,\mathrm{kJ\cdot kg^{-1}}$. For a detailed discussion of the melting enthalpy of nickel, see Ref. 16.

At the onset of melting, which is indicated with a vertical dotted line in Fig. 4, we obtain a value of $0.576\,\mu\Omega\cdot\mathrm{m}$ for the electrical resistivity of nickel, and at the end of melting, a value of $0.772\,\mu\Omega\cdot\mathrm{m}$; thus, an increase of $\Delta\rho = 0.196\,\mu\Omega\cdot\mathrm{m}$ at melting is observed. Cezairliyan and Miiller [29] report $\rho(1700\,\mathrm{K}) = 0.596\,\mu\Omega\cdot\mathrm{m}$ for the solid phase, Hixson et al. [22] report $\rho_{\mathrm{IG}}(1729\,\mathrm{K}) = 0.937\ \mu\Omega\cdot\mathrm{m}$, and Seifter [18] has measured $\rho_{\mathrm{IG}}(1729\,\mathrm{K}) = 0.790\,\mu\Omega\cdot\mathrm{m}$.

The measured values show good agreement with literature values for the solid phase, whereas in the liquid phase there is more scatter in the data. It should be noted that recent measurements tend to lower resistivity values in the liquid phase, even when compared to earlier measurements at the same laboratory [16, 18]. Up to now, we could not find a reasonable explanation for this behavior, as other materials, e.g., molybdenum [31] that also have been recently re-measured, did not show such discrepancies in the liquid resistivity data.

In the temperature range $1420\,\mathrm{K} < T < 1790\,\mathrm{K}$ we obtain for solid iron a c_p of $728.8\,\mathrm{J\cdot kg^{-1}\cdot K^{-1}}$, and for the liquid in the temperature range $1830\,\mathrm{K} < T < 2370\,\mathrm{K}$, a c_p value of $766.4\,\mathrm{J\cdot kg^{-1}\cdot K^{-1}}$; literature values are $c_p(1800\,\mathrm{K}) = 799\,\mathrm{J\cdot kg^{-1}\cdot K^{-1}}$ from Cezairliyan and McClure [6] and $c_p\ (1809\,\mathrm{K}) = 824.7\,\mathrm{J\cdot kg^{-1}\cdot K^{-1}}$ from Hultgren et al. [32]. The measured values are in good agreement with literature values.

As shown in Fig. 5, we obtain a value of $(238 \pm 19)\,\mathrm{kJ\cdot kg^{-1}}$ for the melting enthalpy ΔH, and Hultgren et al. [10] recommend $247\,\mathrm{kJ\cdot kg^{-1}}$. For a detailed discussion of the melting enthalpy of iron, see Ref. 23.

At the onset of melting, which is indicated with a vertical dotted line in Fig. 6, we obtain a value of $1.244\,\mu\Omega\cdot\mathrm{m}$ for the electrical resistivity of iron, and at the end of melting, a value of $1.275\,\mu\Omega\cdot\mathrm{m}$; thus, an increase of $\Delta\rho = 0.031\ \mu\Omega\cdot\mathrm{m}$ at melting is observed. Cezairliyan and McClure [6] report $\rho_{IG}(1800\,\mathrm{K}) = 1.269\,\mu\Omega\cdot\mathrm{m}$ for the solid phase, and Beutl et al. [23] report $\rho_{IG}(1808\,\mathrm{K}) = 1.29\,\mu\Omega\cdot\mathrm{m}$ for the liquid. Our values are in good agreement with literature values, but as mentioned above, recent measurements in the liquid phase tend to lower resistivity values.

5. UNCERTAINTY

According to the guide to the expression of uncertainty in measurements [33] uncertainties reported here are expanded relative uncertainties with a coverage factor of $k = 2$. An evaluated set of uncertainties is given; for the measured pulse-heating data, the following uncertainties are estimated: current, I, 2%; voltage drop, U, 2%; temperature, T, 4%; mass m, 2%, from which we obtain for enthalpy, H, 4%; enthalpy of melting ΔH, 8%; specific heat capacity c_p, 8%; specific electrical resistivity with initial geometry, $\rho_{el,IG}$, 4%, and specific electrical resistivity with volume expansion considered, $\rho_{\mathrm{el,VOL}}$, 6%. The corresponding expanded uncertainties are indicated on the figures.

For the DSC data the uncertainties are as follows: temperature, T, 2 K; and specific heat capacity, c_p, 3%. The uncertainties of the temperature values after the merging of pulse-heating and DSC data results are dominated by the uncertainty of the enthalpy values obtained by pulse-heating. Out of this, the uncertainty over the whole temperature interval is estimated in Figs. 2, 4, and 6 with 4%.

6. CONCLUSION

In this study the temperature dependencies of the enthalpy and electrical resistivity of the metals Fe, Ni, and Pt have been reported and compared to literature values. The temperature dependencies could be

extrapolated down to a temperature of about 500 K. Despite the different heating rates, both methods used here give very good agreement of the obtained thermophysical data within the stated uncertainties of each experiment. The fast pulse-heating technique can suppress phase transformations in the solid phase [34] and allows measurements in metastable phases. Therefore, one has to be very careful in data evaluation, and all data have to be compared with quasi-static methods. For pure metals, melting establishes equilibrium, and in the liquid phase, the values will be again close to thermodynamic equilibrium.

ACKNOWLEDGMENT

This work was supported by the "Fonds zur Förderung der wissenschaftlichen Forschung", Grant No. P15055.

REFERENCES

1. E. Kaschnitz, G. Pottlacher, and H. Jäger, *Int. J. Thermophys*. **13**:699 (1992).
2. G. Pottlacher, E. Kaschnitz, and H. Jäger, *J. Non-Cryst. Solids* **156–158**:374 (1993).
3. C. Cagran, C. Brunner, A. Seifter, and G. Pottlacher, *High Temps. High. Press*. **34**:669 (2002).
4. A. Cezairliyan, J. L. McClure, and C. W. Beckett, *J. Res. Nat. Bur. Stand. (U.S.)* **75A**:1 (1971).
5. A. Cezairliyan and A. P. Miiller, *Int. J. Thermophys.* **5**:315 (1984).
6. A. Cezairliyan and J. L. McClure, *J. Res. Nat. Bur. Stand. (U.S.)* **78A**:1 (1974).
7. T. Baykara, R. H. Hauge, N. Norem, P. Lee, and J. L. Margrave, *High Temp. Sci*. **32**:113 (1991).
8. R. S. Hixson and M. A. Winkler, *Int. J. Thermophys*. **14**:409 (1993).
9. M. M. Martynyuk and V. I. Tsapkov, *Fiz. Metal. Metalloved*. **37**:49 (1974).
10. R. Hultgren, P. D. Desai, D. T. Hawkins, M. Gleiser, K. K. Kelley, and D. D. Wagman, *Selected Values of the Thermodynamic Properties of the Elements* (American Society for Metals, Materials Park, Ohio, 1973).
11. V. E. Zinov'yev, *Metals at High Temperatures – Standard Handbook of Properties*, National Standard Reference Data Service of the USSR (Hemisphere, New York, 1990).
12. G. R. Gathers, J. W. Shaner, and W. M. Hodgson, *High Temps. – High Press*. **11**: 529 (1979).
13. W. Blanke, *Thermophysikalische Stoffdaten* (Springer Verlag, Berlin, 1989).
14. F. Righini and A. Rosso, *High Temp. – High Press*. **12**:335 (1980).
15. K. C. Mills, B. J. Monaghan, and B. J. Keene, *Thermal Conductivities of Molten Metals – Part 1: Pure Metals*, NPL Report CMMT(A) 53 (1997).
16. W. Obendrauf, E. Kaschnitz, G. Pottlacher, and H. Jäger, *Int. J. Thermophys.* **14**:417 (1993).
17. G. Pottlacher, H. Jäger, and T. Neger, *High Temps. – High Press.* **19**:19 (1987).
18. A. Seifter, Ph.D. thesis, TU-Graz, Austria 156 (http://iep.tu-graz.ac.at/thermo) (2001).

19. K. D. Maglic, A. S. Dobrosavljevic, and N. Lj. Perovic, *Thermal Conductivity 20* D, P. Hasselman, ed. (Plenum, New York, 1988), pp. 81–91.
20. Y. S. Touloukian, *Properties of Selected Ferrous Alloying Elements*, CINDAS Data Series on Material Properties–**III**–1 (McGraw-Hill, New York, 1971).
21. U. Seydel and W. Fucke, *Z. Naturforsch.* **32a**:994 (1977).
22. R. S. Hixson, M. A. Winkler, and M. L. Hodgdon, *Phys. Rev. B* **42**:6485 (1990).
23. M. Beutl, G. Pottlacher, and H. Jäger, *Int. J. Thermophys.* **15**:1323 (1994).
24. Y. S. Touloukian, R. W. Powell, C.Y. Ho, and P. G. Klemens, eds., *Thermophysical Properties of High Temperature Solid Materials* – **1** -PT 1 (MacMillan, New York, 1967).
25. A. Cezairliyan and J. L. McClure, *J. Res. Nat. Bur. Stand. (U.S.)* **78a**:1 (1973).
26. A. H. Seville, *J. Chem. Thermodyn*. **7**:383 (1975).
27. J. L. Margrave, *High Temps. – High Press*. **2**:583 (1970).
28. A. K. Chaudhuri, D. W. Bonell, L. A. Ford, and J. L. Margrave, *High Temp. Sci*. **2**:203 (1970).
29. A. Cezairliyan and A. P. Miiller, *Int. J. Thermophys*. **4**:289 (1983).
30. C. Brunner, *Diploma Thesis*, TU-Graz, Austria (http://iep.tu-graz.ac.at/thermo) (2002).
31. C. Cagran, B. Wilthan and G. Pottlacher, *Int. J. Thermophys*. **25**:1551 (2004).
32. R. Hultgren, P. D. Desai, D. T. Hawkins, M. Gleiser, K. K. Kelley, and D. D. Wagman, *Selected Values of the Thermodynamic Properties of the Elements*, American Society for Metals, UMI, Reprinted (1990).
33. Expression of the Uncertainty of Measurement in Calibration, EA-4/02, http://www.european-accreditation.org/pdf/EA-4-02ny.pdf (1999).
34. A. Seifter, G. Pottlacher, H. Jäger, G. Groboth, and E. Kaschnitz, *Ber. Bunsenges. Phys. Chem*. **102**:1266 (1998).